

## POWER CONTROL OF A BIDIRECTIONAL DC BUS FOR FUEL CELLS APPLICATIONS

ANDRÉS FERNANDO RESTREPO\*  
CARLOS ANDRÉS RAMOS-PAJA\*\*  
EDINSON FRANCO\*\*\*

### ABSTRACT

This paper proposes a power system for fuel cell applications able to transfer energy from the power source to the load, and to charge an auxiliary storage device using regenerative power flows generated by the load. The solution is based on a closed loop bidirectional DC/DC converter, where additional devices have been also designed to experimentally test the solution in a safe and realistic environment: a fuel cell emulator and an electronic load.

KEY WORDS: regenerative power flow; DC-DC bidirectional converter; auxiliary storage; electronic load; fuel cell emulator.

## CONTROL DE POTENCIA DE UN BUS DC BIDIRECCIONAL PARA APLICACIONES DE PILAS DE COMBUSTIBLE

### RESUMEN

Este artículo propone un sistema de potencia para aplicaciones de pilas de combustible capaz de transferir energía de la fuente de potencia a la carga y de cargar un sistema de almacenamiento con flujos regenerativos de potencia desde la carga. La solución está basada en un convertidor bidireccional DC/DC en lazo cerrado. Además,

---

\* Ingeniero Electrónico y Magíster en Ingeniería con énfasis en Automática, Universidad del Valle. Profesor e integrante del Grupo de Investigación en Control Industrial (GICI), Universidad del Valle. Cali, Colombia. andres.restrepo@correounivalle.edu.co

\*\* Ingeniero Electrónico y Magíster en Automática, Universidad del Valle; Máster en Ingeniería Electrónica y Doctor en Electrónica de Potencia, Universidad Rovira i Virgili. Profesor Asociado e integrante del Grupo de Investigación GAUNAL, Universidad Nacional de Colombia. Medellín, Colombia. caramosp@unal.edu.co

\*\*\* Ingeniero Electricista, Magíster en Automática y Doctor en Ingeniería, Universidad del Valle. Investigador integrante del Grupo de Investigación en Control Industrial (GICI), Universidad del Valle. Cali, Colombia. edinson.franco@correounivalle.edu.co

se presentan dispositivos auxiliares diseñados para evaluar experimentalmente la solución en un entorno seguro y realista: un emulador de pila de combustible y una carga electrónica.

**PALABRAS CLAVE:** flujo regenerativo; convertidor DC/DC bidireccional; sistema de almacenamiento; carga electrónica; emulador.

## CONTROLE DE POTÊNCIA DE UM ÔNIBUS DC BIDIRECCIONAL PARA APLICAÇÕES DE PILHAS DE COMBUSTÍVEL

### RESUMO

Este artigo propõe um sistema de potência para aplicações de pilhas de combustível capaz de transferir energia da fonte de potência à carga e de carregar um sistema de armazenamento com fluxos regenerativos de potência desde a carga. A solução está baseada em um conversor bidireccional DC/DC em laço fechado. Ademais, apresentam-se dispositivos auxiliares desenhados para avaliar experimentalmente a solução em um meio seguro e realista: um emulador de pilha de combustível e uma carga eletrônica.

**PALAVRAS-CÓDIGO:** fluxo regenerativo; conversor DC/DC bidireccional; sistema de armazenamento; carga eletrônica; emulador.

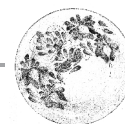
### 1. INTRODUCTION

Fuel cells are power sources that generate electricity from chemical species in an efficient and clean way. In particular, proton exchange membrane fuel cells (PEMFC) are under intense development due to its low operation temperature, high efficiency, and high energy density (Pukrushpan, Stefanopoulou and Peng, 2004a). PEM fuel cells use oxygen ( $O_2$ ) and hydrogen ( $H_2$ ) as reagents that make such devices ideal for automotive applications (Calderón and Mesa, 2004).

In automotive cases, and in general mobile applications, the fuel cells devices operate with regenerative power flows since the load is normally non-constant (Thounthong, Rael and Davat, 2006, 2007), therefore it is necessary to develop power electronic devices able to store and manage multiple power flows: in normal operation the fuel cell must provide the energy required by the load, and in regenerative mode the load provides energy to the system that must be stored in an auxiliary device since the fuel cell is not a reversible device. Moreover, the energy stored in the auxiliary device must be able to be used to provide energy to the load.

Such a topic has been addressed in literature by using different storage devices: Thounthong, Rael and Davat (2007) developed a regulated DC bus for a hybrid vehicle, where a PEMFC is the main power source (Pukrushpan, Stefanopoulou and Varigonda, 2004; Real, Arce and Bordons, 2007) and a bidirectional DC/DC converter is used to manage the power flows, while supercapacitors are adopted to implement the auxiliary storage system. In a similar way, the solution proposed in this paper provides the required power flow management between the fuel cell, the auxiliary storage device, and the load, by means of a specialized closed-loop switching converter, which has been experimentally validated. In addition, auxiliary devices have been developed to perform safe and realistic experiments: a fuel cell emulator and an electronic load, whose circuits and implementation are discussed in detail. Finally, the proposed bidirectional device and its auxiliary test system provide an experimental platform to test automotive power control techniques and optimization algorithms.

The paper presents the experimental power system structure, where the fuel cell emulation sys-



tem, the proposed bidirectional DC/DC converter, and electronic load are described in detail. In addition, the auxiliary storage device is introduced, and the integration of the complete system is validated by means of experimental tests. Finally, the analysis and design of the bidirectional system (Ortúzar, 2002) implemented to manage the power flows is one of the most interesting contributions of this work. Conclusions close the paper.

## 2. POWER SYSTEM DESCRIPTION

The bidirectional power flow system, depicted in figure 1, provides two operating modes: the first one allows to supply the load from the fuel cell or the auxiliary storage device, while the second one permits to charge the storage device using regenerative power flows from the load. The system main components are the bidirectional DC/DC converter, the power source consisting of an experimentally validated fuel cell emulator, an electronic load to impose power consumption profiles, and the auxiliary storage device. The following subsections describe in detail each component of the system.

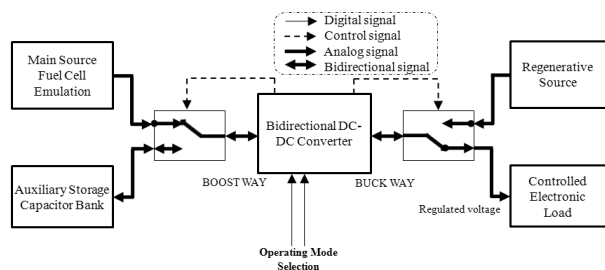


**Figure 1.** Block diagram of the bidirectional power flow system

### 2.1 Fuel cell emulation system

The adopted fuel cell system model is based on the 1,2 kW Nexa power module from Ballard Power Systems, which has been accurately analyzed by Pukrushpan, Stefanopoulou and Peng (2004b) and by Real, Arce and Bordons (2007) taking into account its multiple auxiliary devices. The Nexa fuel

cell has been selected since it is widely accepted in research tasks, and also because it is extensively used in automotive and portable applications. Moreover, the fuel cell exhibits a non-linear current-voltage relation, named polarization curve, therefore its output voltage is not constant and it requires a DC/DC power converter to be interfaced with a regulated DC bus.

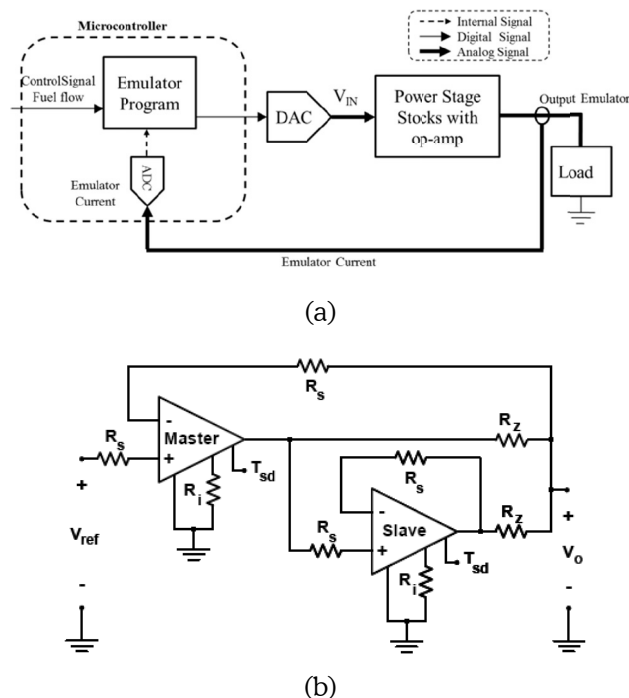


**Figure 2.** Fuel cell emulator: a) block diagram; b) power stage circuitual scheme

The fuel cell stack is the core of the power system, but it is sensitive to high current ripples and derivatives, therefore it must be emulated to avoid damages in the test of power electronics devices (Ramos-Paja *et al.*, 2010a, 2010b). In this way, this paper proposes a fuel cell emulator to test the bidirectional power system and its control strategy: figure 2a shows the block diagram of the fuel cell emulator, where a microcontroller processes the fuel cell model based on the Pukrushpan work, it providing the reference  $V_{IN}$  for the emulator power stage depicted in figure 2b, where Master and Slave devices are high-power operational amplifiers. This emulation system is a closed loop device that measures the load current to provide the modeled fuel cell voltage, where the

current sensing and voltage reference are interfaced by means of analog-to-digital (ADC) and digital-to-analog (DAC) converters. In addition, the emulator is parameterized to reproduce multiple fuel flow conditions defined by a control signal, which permits to use the device to test fuel cell optimization techniques.

The fuel cell model has been parameterized to reproduce the experimental behavior of a EcoFC H2-Economy fuel cell that produces up to 3,5 W at 0,6 V when oxygen at 1 bar and hydrogen at 1,2 bar are provided, it operating at 80 °C. The experimental fuel cell stack is composed by 12 cells in series, and an MTS-150 fuel cell controller regulates the system oxygen and hydrogen flows, and also limits the stack temperature.

The emulator power stage, depicted in figure 2b, is based on a master-slave configuration for two OPA549 operational amplifiers (Texas Instruments, 2005). Such a circuit allows a maximum output current equal to 16 A, this in a balanced output impedance condition achieved by properly selecting  $R_z$  resistances. The voltage regulation is performed by the feedback of the output voltage  $V_o$  to the master OPA549 that makes it equal to the reference voltage  $V_{ref}$  provided by the microcontroller, emulating in this way the fuel cell without any external voltage controller (Ramos-Paja *et al.*, 2010a), reducing the system complexity and cost.

The emulator provides output voltages within [0, 12] V and currents within [0, 12] A. Such specifications make this emulator able to represent PEMFC composed by 1 to 12 cells in series. The emulator ex-

perimental validation has been performed considering a 12 cells stack since it demands the maximum power available, therefore it allows to test the device in the most critical condition (Ramos-Paja *et al.*, 2009a).

The emulator electrical behavior was validated by contrasting its static characteristics with the ones exhibited by the real H2-Economy fuel cell, as depicted in figure 3a, where a satisfactory reproduction of the experimental data for different fuel flow conditions was achieved. Similarly, figure 3b shows the comparison between the experimental and emulated fuel cell transient responses, which ones depend on the activation, ohmic and concentration effects as described by Pukrushpan, Stefanopoulou and Peng (2002), by Correa *et al.* (2004) and by Pukrushpan, Stefanopoulou and Varigonda (2004). It is noted that step changes in the stack current are directly reflected in the output voltage due to the ohmic effect. The tests depicted in figure 3b were performed by applying an impedance step change in the experimental fuel cell while its current and voltage were registered, then the recorded current profile was applied to the emulator, obtaining satisfactory results. Such an experiment illustrates the inverse relation between stack current and its voltage, therefore it is necessary to adopt a DC/DC power converter able to regulate the system output voltage for any acceptable load current condition (Ramos-Paja *et al.*, 2009b).

Finally, the experimental results confirm the usefulness of the developed fuel cell emulator in the test of power electronics devices without imposing dangerous situations to real fuel cell prototypes, i.e. H2 ECONOMY fuel cell.

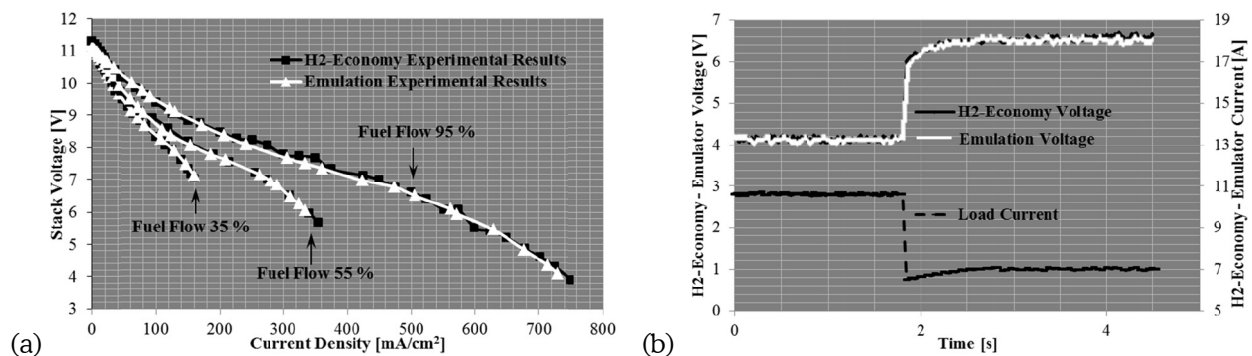
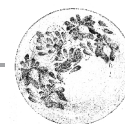


Figure 3. Fuel cell emulator experimental validation: a) polarization curve (V-I); b) dynamic response



## 2.2 Closed loop bidirectional DC/DC switching converter

The adopted bidirectional DC/DC converter is able to transfer energy between its two ports, supporting both positive and negative currents. Most of the DC/DC converters topologies, with and without galvanic isolation, are suitable to be used as bidirectional converters by substituting the diodes by properly regulated MOSFETs (Flores, 2004).

Figure 4 shows the bidirectional boost-buck converter used to increase the voltage from input  $V_1$ , i.e. fuel cell or auxiliary storage device, to the DC bus voltage level  $V_2$ . Such a converter also supports the inverse power flow in buck operation mode from  $V_2$  (DC bus or regenerative load) to  $V_1$  (auxiliary storage device). The MOSFET used in the converter was a N-channel IRF540N from International Rectifier. It is noted that S1 and S2 MOSFETs activation are complementary to avoid fuel cell short-circuits: in boost mode the S1 MOSFET is the independent one and S2 is activated by a complementary signal, while in buck mode the S2 MOSFET is the independent one and S1 is activated by a complementary signal.

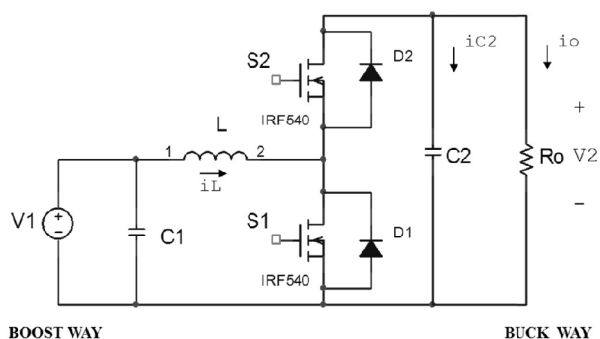


**Figure 4.** Bidirectional buck-boost DC/DC switching converter

The bidirectional converter is controlled by means of a 20 kHz PWM (Pulse Width Modulation), and its control structure is depicted in figure 5; depending on the required power flow direction, the microcontroller drives S1 and S2 MOSFETs by means of a PID controller. In addition, the converter passive elements were calculated to fulfill the fuel

cell small current ripple requirement (Erickson and Maksimovic, 2001) considering a DC bus voltage equal to 12 V, and fuel cell and auxiliary storage voltages within the range [3,5-11,5] V. The nominal power of the converter is then 50 W, and its inductor design ensures a continuous conduction mode (CCM) (Mohan, Undeland and Robbins, 2003) for the adopted operating conditions. The converter parameters are:  $L = 450 \mu\text{H}$ ,  $C_1 = 2200 \mu\text{F}$ ,  $C_2 = 2200 \mu\text{F}$  and  $R_o = 47 \Omega$ .

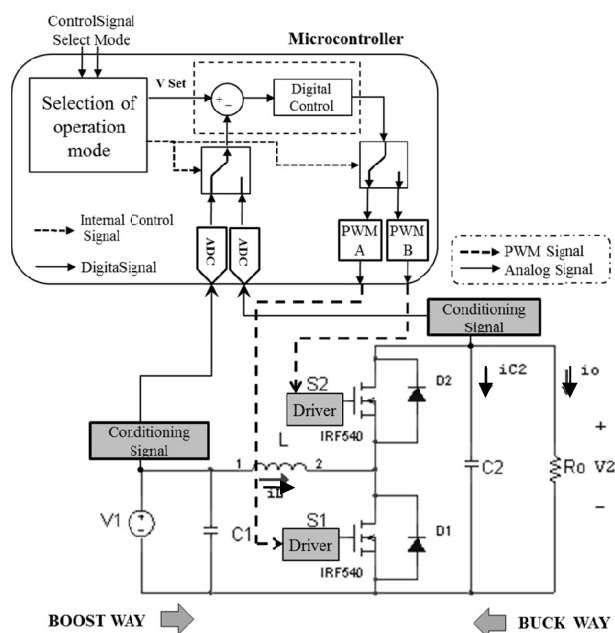


**Figure 5.** DC/DC converter control structure

The converter was controlled by using an ATmega16 microcontroller (Atmel Corporation, 2008), where the input and output port voltages are measured to calculate the control signal as in (1)-(2). In such equations  $e$  represents the error signal used to process the PID controller,  $v_{ref}$  represents the desired voltage, and  $v_{me}$  represents the measured voltage: DC bus or load voltage for the boost mode, and auxiliary storage or fuel cell voltage for the buck mode. The error signal is calculated in each duty cycle period, as well as the control command that defines the converter duty cycle generated by the PID structure given in (2), where  $K_p$  is the proportional constant,  $K_i$  the integral constant and  $K_d$  the derivative constant.

$$e = v_{ref} - v_{me} \quad (1)$$

$$C(t) = Kp * e(t) + Ki * \int_0^t e(t) * dt + Kd * \frac{de(t)}{dt} \quad (2)$$

Since the ATmega16 microcontroller process only digital equations, the analogue controller given in (2) has been digitalized in difference equations as given in (3), where  $T_i = 1/K_i$  represents the integral time constant,  $T_d = K_d$  the derivative time constant, and  $T_s$  the sampling time.

$$C(n) = Kp * e(n) + \frac{T_s}{T_i} * \sum_0^N e(n) + \frac{T_d}{T_s} * [e(n) - e(n-1)] \quad (3)$$

The controller parameters were designed by means of the root-locus placement technique (Erickson and Maksimovic, 2001) by using the small signal models of both boost and buck circuits. In this way, the small-signal model of the boost converter (Ramos-Paja *et al.*, 2009b) is:

$$\begin{bmatrix} \hat{x}_1(s) \\ \hat{x}_2(s) \end{bmatrix} = \begin{bmatrix} s + \frac{1}{RoC2} & -\frac{(1-D)}{L} \\ \frac{(1-D)}{C2} & s \end{bmatrix} * \begin{bmatrix} \frac{1}{L} & 0 \\ 0 & \frac{1}{C2} \end{bmatrix} * \begin{bmatrix} \hat{u}_1(s) \\ \hat{u}_2(s) \end{bmatrix} + \begin{bmatrix} \frac{X_{20}}{L} \\ -\frac{X_{10}}{C2} \end{bmatrix} * \hat{d}(s) \quad (4)$$

where  $x_1$  represents the inductor current,  $x_2$  the C2 capacitor voltage,  $u_1$  the input voltage (main or auxiliary power source),  $u_2$  models the load perturbations,  $d$  and  $D$  represents the converter small-signal and steady-state duty cycle values, respectively. In such a model the capital letters denote steady-state values, and the small-signal single input-single output transfer function between the output voltage  $\hat{x}_2$  and the duty cycle  $\hat{d}$  is:

$$\frac{\hat{x}_2(s)}{\hat{d}(s)} = \frac{(1-D) * X_{20} - s * \frac{X_{10}}{C2}}{s^2 + \frac{s}{RoC2} + \frac{(1-D)^2}{LC2}} \quad (5)$$

The controller designed for this operating mode has the following parameters:  $K_p = 0,3$ ;  $K_i = 0,001$ ;  $K_d = 0$ ; this with a  $T_s = 2$  ms.

In a similar way, the small-signal model of the buck converter is given by (6), where  $x_1$  represents the inductor current,  $x_2$  the C1 capacitor voltage, and  $u_1$  the input voltage. Equation 7 gives the small-signal single input-single output transfer function between the output voltage  $\hat{x}_2$  and the duty cycle  $\hat{d}$  used to design the following controller parameters:  $K_p = 0,25$ ;  $K_i = 0,0001$ ;  $K_d = 0$ ;  $T_s = 2$  ms.

$$\begin{bmatrix} \hat{x}_1(s) \\ \hat{x}_2(s) \end{bmatrix} = \begin{bmatrix} s + \frac{1}{RoC1} & -\frac{1}{L} \\ \frac{1}{C1} & s \end{bmatrix} * \begin{bmatrix} \frac{D}{L} \\ 0 \end{bmatrix} * \begin{bmatrix} \hat{u}_1(s) \\ \hat{d}(s) \end{bmatrix} + \begin{bmatrix} \frac{U_{10}}{L} \\ 0 \end{bmatrix} * \hat{d}(s) \quad (6)$$

$$\frac{\hat{x}_2(s)}{\hat{d}(s)} = \frac{\frac{U_{10}}{LC1}}{s^2 + \frac{s}{RoC1} + \frac{1}{LC1}} \quad (7)$$

The closed loop bidirectional DC/DC converter has been experimentally tested in both boost and buck modes. The boost mode was evaluated by defining a regulated 12 VDC bus voltage, where perturbations on the DC bus current and power source voltage, i.e. fuel cell or auxiliary storage device, were applied. The test defines a DC bus impedance equal to 47  $\Omega$ , and low frequency variations between 11,3 V and 3,5 V were applied to the input port voltage, which are typical on fuel cells and high capacitive storage devices. In such conditions the system behavior is satisfactory as reported in figure 6a, where the DC bus voltage is accurately regulated in presence of the input voltage perturbations. An additional experiment was performed in boost mode by defining a constant input port voltage equal to 9 V and applying perturbations to the DC bus impedance: it starts at 47  $\Omega$ , then it is decreased to 4,52  $\Omega$ , and finally it is further reduced to 3,11  $\Omega$ . This test evaluates the performance of the converter and its controller in load perturbations. The experimental results are depicted in figure 6b, where it is observed the satisfactory response of the closed loop converter in the DC bus voltage regulation.

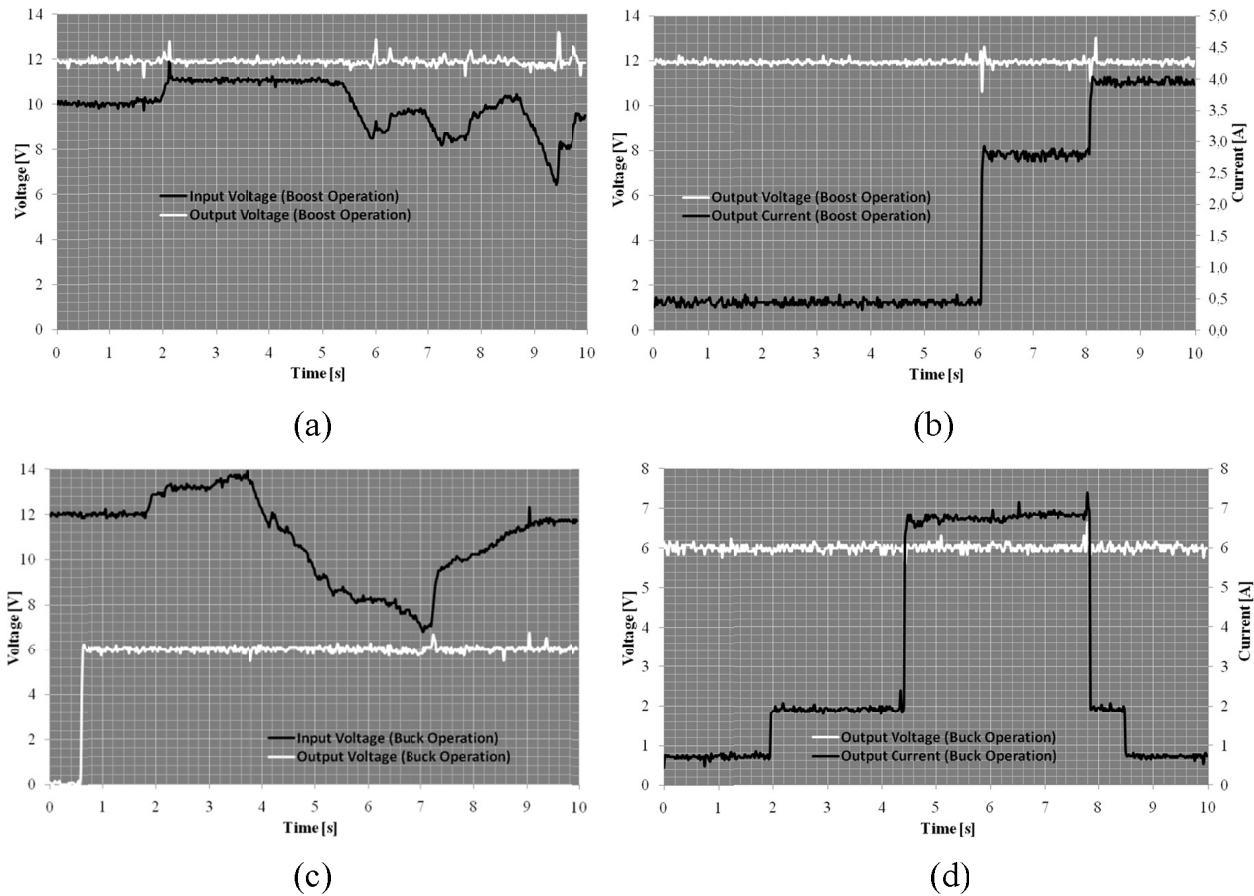


**Figure 6.** Experimental dynamic response of the closed loop bidirectional converter: a) boost mode with input voltage transient; b) boost mode with load current transient; c) buck mode with input voltage transient; d) buck mode with load current transient

The buck mode was also tested, where the first experiment considers an input port V1 voltage equal to 6 V, i.e. auxiliary storage device, meanwhile low-frequency DC bus voltage perturbations are applied within [6,4-14] V, by adopting an auxiliary storage device impedance equal to 10  $\Omega$ . Figure 6c shows the experimental results, where it is noted the satisfactory bus voltage regulation. Similarly, an additional test adopting a constant 12 VDC bus and a desired V1 voltage equal to 6 V is performed, by considering changes in the impedance of the auxiliary storage device: it starts at 10  $\Omega$ , then it is reduced to 3,33  $\Omega$ , and finally it is further decreased to 0,88  $\Omega$ , where figure 6d exhibits the satisfactory results achieved in such transient conditions.

Finally, it is noted that in the boost operating mode the steady-state voltage error is lower than 0,8 %, while in buck mode it is lower than 0,3 %. Such experimental results illustrate the accurate regulation of the device.

### 2.3 Regulated electronic load

An electronic load was developed to experimentally test the system under typical load profiles in portable devices, automotive applications, DC/DC converters, and in general to reproduce the behavior of a desired load device (Wang, Hou and Peng, 2009; Zhang *et al.*, 2009). It is noted that several commercial electronic loads are available, but they are

costly devices, normally over-dimensioned for low power applications. Therefore, this paper proposes a simple and low-cost electronic load for low power applications, up to 60 W, which is based on a closed loop MOSFET in its linear operating zone (Zhang and Chen, 2006; Wang *et al.*, 2010). This electronic load operates as a voltage controlled ( $V_{GS}$ ) current source ( $I_{load}$ ), where the adopted MOSFET was an International Rectifier N-channel IRFP32N50K. An important parameter used to select the MOSFET concerns its turn-on gate voltage ( $V_{GS(ON)}$  or  $V_{GS(th)}$ ). Such a parameter depends on the manufacturer (International Rectifier, 2004) and it defines the minimum control signal that must be applied to the MOSFET. The IRFP32N50K has  $3\text{ V} < V_{GS(ON)} < 5\text{ V}$ , which is acceptable to adopt a controller implementation based on common operational amplifiers. The proposed solution uses a PI structure to ensure a null steady-state error, where the output current is measured by means of a LEM HX 10-P current sensor.

Since the electronic load operates as a voltage controlled current source, an ATmega16 microcontroller was used to store the desired load profiles in terms of voltage references for the power stage delivered by means of a DAC. The block diagram of the designed electronic load is depicted in figure 7.

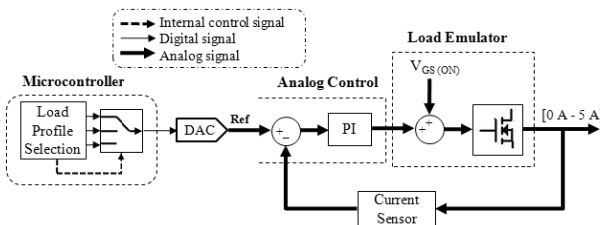


Figure 7. Electronic load block diagram

The electronic load was tested for the interesting range by applying a reference voltage within [1-1,6] V that corresponds to an output current within [0-4] A. Figure 8 shows the experimental response of the electronic load for the tested range, where it is observed its comparison with an ideal linear behavior. The developed device exhibits a small error at low currents where the MOSFET consumption is significant, while a maximum error equal to 1 % is

achieved at 4 A. The small deviation at small currents is also caused by the 40 mV sensitivity exhibited by the LEM HX 10-P current sensor.

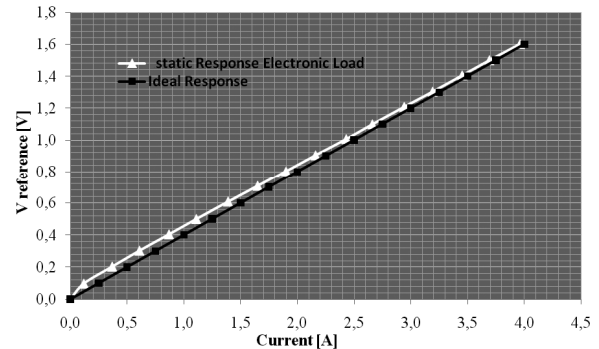


Figure 8. Electronic load experimental test

### 3. BIDIRECTIONAL POWER FLOWS: OPERATING MODES

The proposed platform allows to transfer energy from the main or auxiliary power sources to the load, and from the regenerative load to the storage device. Therefore, two modes have been defined: *consumption mode* and *regenerative mode*. The system block diagram, previously presented in figure 1, is extended in figure 9 to illustrate the physical implementation of the fuel cell emulator, the auxiliary storage device, i.e. capacitor bank, the bidirectional power converter, and the electronic load. In addition, the regenerative load is simulated by means of an external power source coupled with the electronic load, which allows both power consumption and regeneration to the system.

The power required by fuel cell emulator was supplied by an Agilent power source HP-6439B, and a dual power source GPC-3030D from GW Instek was used to provide the load regenerative power, and also to provide power to the control circuits. In addition, the reported experimental data were measured using a GW Instek oscilloscope GDS-2062. Finally, the operating mode of the converter is selected by means of a binary command imposed by an external device, i.e. micro-controller, PLC, etc.



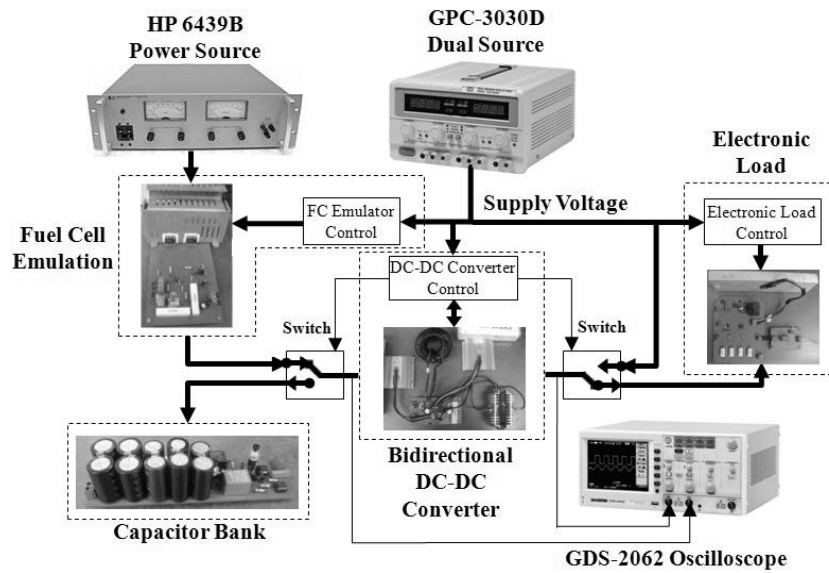
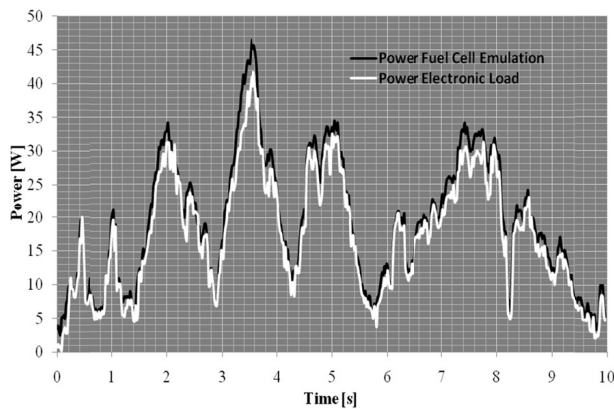


Figure 9. Power system block diagram

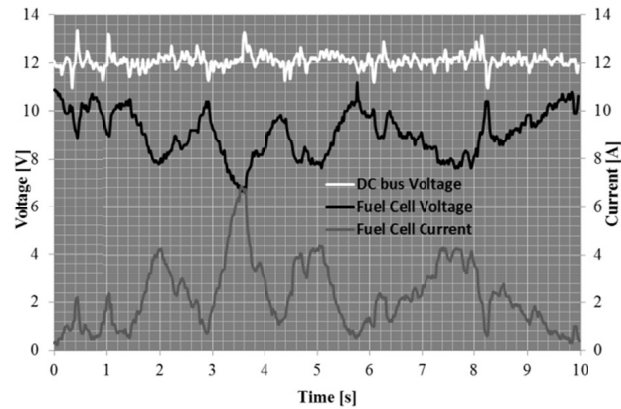
### 3.1 Consumption mode

The consumption mode requires the operation of the bidirectional DC/DC converter in boost mode to transfer energy from the power source, i.e. the fuel cell emulator or auxiliary storage, to the electronic load. In this mode the fuel cell emulator exhibits

different non-linear polarization curves depending on the fuel flow control signal (FF) as depicted in figure 3a, where the fuel cell voltages and currents are constrained to [3,5-11,5] V and [0-12] A, respectively. This boost mode provides an output voltage regulation, i.e. DC bus or load voltage, which in this application has been set to 12 V.



(a)



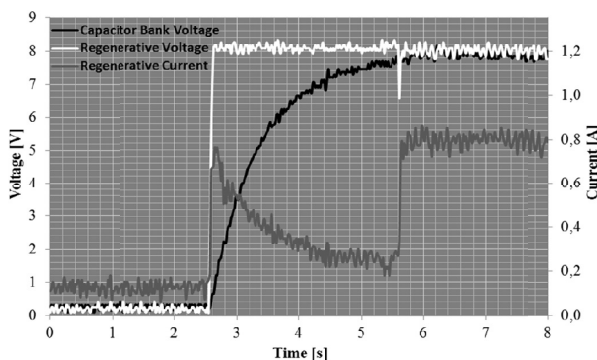
(b)

Figure 10. Experimental consumption mode operation: a) power flows; b) bus regulation in load current transients

This operating mode was experimentally tested using a high frequency load profile based on typical automotive drive profiles (Ed Barger *et al.*, 2003). Figure 10a shows the fuel cell (emulated) and load power profiles, where it is observed the accurately tracking of the requested power, while the difference is generated by the system losses. Similarly, figure 10b shows the satisfactory DC bus voltage regulation achieved when fuel cell voltage and current disturbances are present. It is noted that such disturbances were generated by the load profile given in figure 10a, since as described in figure 3a, load current perturbations cause changes in the fuel cell voltage. Finally, such an experiment illustrates the accurate load bus regulation in consumption mode.

### 3.2 Regenerative mode

This mode requires the operation of the bidirectional DC/DC converter in buck mode to transfer energy from the regenerative load, simulated by means of an external power source, to the auxiliary storage device. Such a storage was developed by using a capacitor bank with 47 mF and 8 V nominal voltage as depicted in figure 9, where an additional 15  $\Omega$  resistance was introduced to constrain the capacitors current, generating a system constant time  $\tau = 0,705$ . The regenerative load imposes an 8 VDC bus voltage, providing energy to the converter. The auxiliary storage voltage is regulated to 8 V.



**Figure 11.** Experimental regenerative mode operation

This buck mode was experimentally tested under the previously described conditions. Figure 11 shows the satisfactory system behavior, where the 8 VDC regenerative voltage is observed. In addition, the capacitors bank voltage is regulated to the desired 8 VDC value in 4,25  $\tau$  while the regenerative load provides power to the system. Finally, this experiment illustrates the satisfactory system behavior in regenerative mode.

### 3.3 Power conversion efficiency

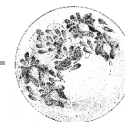
The bidirectional DC/DC converter efficiency was calculated from the comparison of both input and output powers, where the main power losses are caused by the parasitic resistances and semiconductors switching losses. In boost mode the converter exhibits a high efficiency near to 92 % for output power profiles higher than 5 W, which corresponds to the 90 % of the operating range. Similarly, in buck mode (regenerative path) the converter exhibits a high efficiency near to 91 %.

## 4. CONCLUSIONS

The proposed power system is able to transfer both consumption and regenerative power flows from main and auxiliary power sources to the load, and from the load to the storage device. Such a characteristic is very useful in portable applications that allow to extract energy from the load, as electric vehicles.

The methodology to design the power system and its associated controllers was also presented. In addition, supporting devices to test the power system have been specified, designed, and implemented: a fuel cell emulator and an electronic load. Both devices have been experimentally tested, and they provide realistic and safe conditions to test fuel cell intended applications.

Moreover, the implemented power electronics solution exhibits a high electrical efficiency up to 92 %, and its experimental validation shows the



accurate fuel cell protection, DC bus regulation, and satisfactory storage device management for load current perturbations typical in electric vehicle applications. Finally, the solution can be improved by designing an algorithm to perform automatic transitions among modes of the dc/dc converter, it based on the power flows of the hybrid fuel cell/capacitor bank system.

## ACKNOWLEDGEMENTS

This work was supported by GICI group of the Universidad del Valle, Cali, Colombia, under the project "Entorno de aprendizaje basado en proyectos para sistemas de control" (code: 110652128453, contract: 401-2011 Colciencias). The work was also supported by GAUNAL group of the Universidad Nacional de Colombia under the projects SMART-ALEN and VECTORIAL-MPPT.

## REFERENCES

- Atmel Corporation (2008). "8-bit microcontroller with 16K bytes in-system programmable flash, ATmega16, ATmega16L". June, pp. 1-358. [Consulted on March 19, 2010]. Available in: <[http://www.atmel.com/dyn/resources/prod\\_documents/doc2466.pdf](http://www.atmel.com/dyn/resources/prod_documents/doc2466.pdf)>
- Calderón, Marco Tulio y Mesa, Leonardo (2004). "Principios de funcionamiento y construcción de una celda de combustible de ácido fosfórico (PAFC)". *Scientia et Technica*, año X, No. 25 (agosto), pp. 125-130.
- Correa, J. M.; Farret, F. A.; Canha, L. N. and Simoes, M. G. (2004). "An electrochemical-based fuel-cell model suitable for electrical engineering automation approach". *IEEE Transactions on Industrial Electronics*, vol. 51, No. 5 (October), pp. 1105-1106.
- Ed Bargar, H.; Li, J.; Goering, D. J. and Lee J. H. (2003). "Modeling and verification of hybrid electric HMMWV performance". *Industrial Electronics Society 2003*, vol. 1, November 2-6, pp. 939-944.
- Erickson, Robert W. and Maksimovic, Dragan. *Fundamental of power electronics*. 2<sup>nd</sup> ed. United States: Kluwer Academic Publishers, 2001. 883 p. ISBN 079-23-7270-0.
- Flores, Luis Alejandro. *Estudio y análisis de soluciones topológicas de convertidores CC-CC bidireccionales para su aplicación en vehículos híbridos*. Tesis doctoral (Doctor Ingeniero Industrial), Universidad Politécnica de Madrid, Madrid, 2004. 300 p. [consultado el 25 de enero de 2011]. Disponible en: <<http://oa.upm.es/178/01/05200434.pdf>>
- International Rectifier (2004). "HEXFET power MOSFET IRFP32N50K". 8 p. [Consulted on June 26, 2010]. Available in: <<http://www.irf.com/product-info/datasheets/data/irfp32n50k.pdf>>
- Mohan, Ned; Undeland, Tore M. and Robbins, William P. *Power electronics: Converters, applications, and design*. 2 ed. United States: John Wiley & Sons, 2003. 802 p. ISBN 0-471-22693-9.
- Ortúzar, Micah Etan. *Diseño y construcción de convertor DC-DC para control de ultracapacitores en vehículo eléctrico*. Trabajo de grado (Ingeniero Civil Industrial, con Diploma en Ingeniería Eléctrica). Pontificia Universidad Católica de Chile, Santiago de Chile, 2002. 154 p. [consultado el 25 de enero de 2011]. Disponible en: <<http://www2.ing.puc.cl/power/paperspdf/dixon/tesis/Ortuzar.pdf>>
- Pukrushpan, Jay T.; Stefanopoulou, Anna G. and Peng, Huei (2002). *Modeling and control for PEM fuel cell stack system*. Proceedings of the 2002 American Control Conference, Anchorage, AK (8-10 May), vol. 4, pp. 3117-3122.
- Pukrushpan, Jay T.; Stefanopoulou, Anna G. and Peng, Huei. *Control of fuel cell power systems: Principles, modeling, analysis and feedback design*. London: Springer, 2004a. 11 p.
- Pukrushpan, Jay T.; Stefanopoulou, Anna G. and Peng, Huei (2004b). "Control of fuel cell breathing". *IEEE Control Systems Magazine*, vol. 24 (April), pp. 30-46.
- Pukrushpan, Jay T.; Stefanopoulou, Anna G. and Varigonda, Subbarao (2004). *Control oriented model of an integrated fuel cell stack and fuel processor system*. Proceedings of the First IFAC Symposium on Advances in Automotive Systems 2004, Salerno, Italy (19-23 April), vol. 1, pp. 1-6.
- Ramos-Paja, C. A.; Bordons, C.; Romero, A.; Giral, R. and Martinez-Salamero, L. (2009b). "Minimum fuel consumption strategy for PEM fuel cells". *IEEE Transactions on Industrial Electronics*, vol. 56, No. 3 (March), pp. 685-696.
- Ramos-Paja, C. A.; Giral, R.; Martinez-Salamero, L.; Romano, J.; Romero, A. and Spagnuolo, G. (2010b). "A PEM fuel-cell model featuring oxygen-excess-ratio estimation and power-electronics interaction". *IEEE Transactions on Industrial Electronics*, vol. 57, No. 6 (June), pp. 1914-1924.

- Ramos-Paja, C. A.; Romero, A.; Giral, R.; Martinez-Salamero, L. and Sanchez, C. I. (2010a). "Switching and linear power stages evaluation for PEM fuel cell emulation". *International Journal of Circuit Theory and Applications*, vol. 39, No. 5 (March), pp. 475-499.
- Ramos-Paja, C. A.; Romero, A.; Giral, R.; Vidal-Idiarte E. and Martinez-Salamero, L. (2009a). "Fuzzy-based modelling technique for PEMFC electrical power generation systems emulation". *Power Electronics-IET*, vol. 2, No. 3 (May), pp. 241-255.
- Real, Alejandro; Arce, Alicia and Bordons, Carlos (2007). "Development and experimental validation of a PEM fuel cell dynamic model". *Journal of Power Sources*, vol. 173, No.1 (May), pp. 310-324.
- Texas Instruments Incorporated (2005). "High-voltage, high-current operational amplifier OPA549". pp. 1-18. [Consulted on November 8, 2010]. Available in: <<http://focus.ti.com/lit/ds/symlink/opa549.pdf>>
- Thounthong, P.; Rael, S. and Davat, B. (2006). "Control strategy of fuel cell/supercapacitors hybrid power sources for electric vehicle". *Journal of Power Sources*, vol. 158, No. 1 (July), pp. 806-814.
- Thounthong, P.; Rael, S. and Davat, B. (2007). "Control strategy of fuel cell and supercapacitors association for a distributed generation system". *IEEE Transactions on Industrial Electronics*, vol. 54, No. 6 (December), pp. 3225-3233.
- Wang, Shaokun; Hou, Zhenyi and Peng, Chuanbiao (2009). *A repetitive control strategy of AC electronic load with energy recycling*. Proceedings of the Technology and Innovation Conference 2009, Xian, China (October 12-14), pp. 1-4.
- Wang, Zijian; Kong, Feng; Xie, Chaoping and Huang, Zhengwu. (2010). *Design and implementation of the real-time regulation electronic load module based on DSP*. Proceedings of the 2nd International Conference on Future Computer and Communication (ICFCC), 2010, Wuhan, China, vol. 1 (21-24 May), pp. V1-485 - V1-488.
- Zhang, Rong and Chen, Jian (2006). *Repetitive control algorithms for a real-time dynamic electronic load simulator*. Proceedings of the 21th Annual IEEE Applied Power Electronics Conference and Exposition 2006, Dallas TX (March 19-23), pp. 919-928.
- Zhang, Zheyu; Zou, Yunping; Wu, Zhenxing and Tang, Jian (2009). *Design and research of three-phase power electronic load*. Proceedings of the Power Electronics and Motion Control Conference 2009 (May 17-20), pp. 1798-1802.